

Scintillations of cos-Gaussian and annular beams

Halil T. Eyyuboğlu and Yahya Baykal

Department of Electronic and Communication Engineering, Çankaya University, Öğretmenler Caddesi No. 14, Yüzüncüyıl, 06530 Balgat, Ankara, Turkey

Received June 9, 2006; revised July 26, 2006; accepted July 26, 2006;
posted August 3, 2006 (Doc. ID 71777); published December 13, 2006

Based on the generalized beam formulation, we derive the scintillation index and selectively evaluate it for cos-Gaussian and annular beams propagating in weak atmospheric turbulence. Dependence of the scintillation index on propagation length, focusing and displacement parameters, wavelength of operation, and source size are individually investigated. From our graphical outputs, it is observed that a cos-Gaussian beam exhibits lower scintillations and thus has a tendency to be advantageous over a pure Gaussian beam particularly at lower propagation lengths. It is also found that at longer propagation lengths, this advantage switches to the side of the annular beam. Furthermore, the scintillation index of a focused annular beam will be below those of both Gaussian and cos-Gaussian beams starting at earlier propagation distances. When analyzed against source sizes, it is seen that cos-Gaussian beams will offer advantages at relatively large source sizes, while the reverse will be applicable for annular beams. © 2006 Optical Society of America

OCIS codes: 010.1330, 010.1300, 010.3310, 060.4510.

1. INTRODUCTION

Scintillations arising due to turbulence in the atmosphere basically mean fluctuations in the intensity of the received beam. Scintillation is one of the major limiting factors in atmospheric communication and imaging systems operating at optical frequencies and is therefore investigated both theoretically and experimentally by many researchers.^{1–12} Excellent coverage on the results of these contributions is included in the books by Tatarskii,¹³ Ishimaru,¹⁴ Andrews and Phillips,¹⁵ and Andrews *et al.*¹⁶ In these studies, fundamental laws of intensity fluctuations of optical waves in turbulent atmosphere in the regimes of both weak and strong turbulence have been investigated in detail. The results produced from these studies mainly concern the Gaussian beam wave and the limiting cases, namely, spherical and plane waves. Regarding the scintillations for other types of beams, collimated annular beams are reported by Vetelino and Andrews¹⁷ and flattened beams are presented by Cowan *et al.*¹⁸ Evaluations of the scintillation index for other types of beams, in general, and cos-Gaussian beams and focused annular beams, in particular, do not yet exist in the literature.

In our recent studies, we have introduced different types of incident beams in turbulent atmosphere. Lately, we have presented the formulation of the correlations for general beam types.¹⁹ As special case solutions, by using the formulation presented in Ref. 19, we are able to find the scintillation index of cos-Gaussian, annular beams, and numerous other types of incidences. We have also investigated the scintillation index of flat-topped Gaussian beams²⁰ and extended our fourth-order solutions in turbulence to provide the intensity fluctuations of incident beams exhibiting arbitrary field profiles.²¹ The purpose of these undertakings has been to assess the performance of various types of source beam incidences that can be employed in broadband access free space optics links. The

primary objective here is to see whether these beams would provide advantages when compared to the already known case of a Gaussian beam. In this respect, we have shown²⁰ that flat-topped beams possess better scintillation characteristics than the fundamental Gaussian beam beyond the Fresnel zone. The present paper constitutes the continuation of such efforts in this direction illustrating that cos-Gaussian and focused annular beams may pose other alternatives. In this paper, within the framework of the general beam formulation, for one particular case, we recalculate the scintillation index of flat-topped Gaussian beams thus verifying our earlier results and simultaneously establishing comparisons between flat-topped, annular, and cos-Gaussian beams.

2. FORMULATION

The propagation geometry, relevant to our study, consists of source and receiver planes lying perpendicular to the axis of propagation, z . On the source plane, the position is designated by the vector $\mathbf{s}=(s_x, s_y)$, while the receiver plane vectorial position designator is $\mathbf{p}=(p_x, p_y)$. A general source beam centered with respect to the point $s_x=s_y=0$ will have a field distribution of¹⁹

$$u_s(\mathbf{s}) = u_s(s_x, s_y) = \sum_{l=1}^N \sum_{(n,m)} A_{l,n,m} \exp(-i\theta_{l,n,m}) H_n(a_{xln}s_x + b_{xln}) \times \exp[-(0.5k\alpha_{xln}s_x^2 + iV_{xln}s_x)] H_m(a_{ylm}s_y + b_{ylm}) \times \exp[-(0.5k\alpha_{ylm}s_y^2 + iV_{ylm}s_y)], \quad (1)$$

$A_{l,n,m}$ and $\theta_{l,n,m}$ are, respectively, the amplitude and the phase of the lnm component of the source field; $H_n(a_{xln}s_x + b_{xln})$ and $H_m(a_{ylm}s_y + b_{ylm})$ are the Hermite polynomials defining the beam distribution for s_x and s_y directions, where n and m are the order; a_{xln} and a_{ylm}

stand for the width; b_{xln} and b_{yln} are the complex displacement parameters;

$$\alpha_{xln} = 1/(k\alpha_{sxl n}^2) + i/F_{xln}, \quad \alpha_{yln} = 1/(k\alpha_{sylv n}^2) + i/F_{yln}, \quad (2)$$

where $\alpha_{sxl n}$ and $\alpha_{sylv n}$ are Gaussian source sizes; F_{xln} and F_{yln} are the source focusing parameters along s_x and s_y directions; and $k=2\pi/\lambda$ is the wavenumber with λ being the wavelength and $i=(-1)^{0.5}$. V_{xln} and V_{yln} are the complex parameters used to create physical location displacement and phase rotation for the source field or a combination of both and are simply termed as displacement parameters within the context of the present study. Furthermore, by appropriately setting them as purely real or imaginary quantities and implementing a summation over two terms, i.e., $N=2$, we are able to attain sinusoidal and hyperbolic Gaussian beams.¹⁹ For cos-Gaussian beams, only real values are assigned to displacement parameters.

The detailed steps of acquiring the log-amplitude correlation function, $B_\chi(\mathbf{p}, L)$, on a receiver plane located at a distance $z=L$ from the source plane, for a general beam, are described in Ref. 19. Below, we continue by utilizing the results of this earlier work. From Ref. 19, importing Eq. (13), which corresponds to the correlation function of log-amplitude fluctuations and multiplying this function by 4, we obtain the scintillation index m^2 in weak turbulence as follows:

$$m^2 = 4\pi \operatorname{Re} \left\{ \int_0^L d\eta \int_0^\infty \kappa d\kappa \int_0^{2\pi} d\theta [G_1(\mathbf{p}, L, \eta, \kappa, \theta) + G_2(\mathbf{p}, L, \eta, \kappa, \theta)] \Phi_n(\kappa) \right\}, \quad (3)$$

Here, Re denotes the real part, η is the distance variable along the propagation axis, $\kappa \exp(i\theta)$ is the two-dimensional spatial frequency in polar coordinates, $\Phi_n(\kappa)$ is the spectral density of the index-of-refraction fluctuations. Equations (15)–(26) of Ref. 19 supply the expressions for $G_1(\mathbf{p}, L, \eta, \kappa, \theta)$ and $G_2(\mathbf{p}, L, \eta, \kappa, \theta)$ and the related definitions. They are rewritten below for the zeroth-order on-axis case and for the x - y symmetric alpha parameter, i.e., $n=m=0$, $p_x=p_y=0$, and thus omitting n , m notation, we have $\alpha_{xl}=\alpha_{yl}=\alpha_l=1/(k\alpha_{sl}^2)+i/F_l$, which in turn yield

$$G_1(\mathbf{p}, L, \eta, \kappa, \theta) = \frac{G_N(\mathbf{p}, L, \eta, \kappa, \theta) G_N(\mathbf{p}, L, \eta, -\kappa, \theta)}{D^2(\mathbf{p}, L)}, \quad (4)$$

$$G_2(\mathbf{p}, L, \eta, \kappa, \theta) = \frac{G_N(\mathbf{p}, L, \eta, \kappa, \theta) G_N^*(\mathbf{p}, L, \eta, \kappa, \theta)}{|D(\mathbf{p}, L)|^2}, \quad (5)$$

$$G_N(\mathbf{p}, L, \eta, \kappa, \theta) = \sum_{l=1}^N A_l e^{-i\theta_l} \frac{ik}{(1+i\alpha_l L)} \exp \left[-\frac{i(V_{xl}^2 + V_{yl}^2)L}{2k(1+i\alpha_l L)} \right] \times \exp \left[\frac{i(L-\eta)(V_{xl} \cos \theta + V_{yl} \sin \theta)\kappa}{k(1+i\alpha_l L)} \right] \times \exp \left[-\frac{0.5i(L-\eta)(1+i\alpha_l \eta)\kappa^2}{k(1+i\alpha_l L)} \right], \quad (6)$$

$$D(\mathbf{p}, L) = \sum_{l=1}^N A_l e^{-i\theta_l} \frac{1}{(1+i\alpha_l L)} \exp \left[-\frac{i(V_{xl}^2 + V_{yl}^2)L}{2k(1+i\alpha_l L)} \right]. \quad (7)$$

Note that the above notion implies that x - y symmetry has only been assumed for the source size and the focusing parameters—these are α_{sl} and F_l —whereas the displacement parameters, V_{xl} and V_{yl} , are allowed to be asymmetric in x - y .

By substituting Eqs. (6) and (7) into Eqs. (4) and (5), and by setting $\Phi_n(\kappa)=0.033C_n^2\kappa^{-11/3}$, i.e., Kolmogorov spectrum, C_n^2 being the structure constant, and performing the θ integration of Eq. (3) using Eq. 3.937.2 of Ref. 22 (for $a=b=m=0$), which is $\int_0^{2\pi} d\theta \exp(p \cos \theta + q \sin \theta) = 2\pi I_0[(p^2+q^2)^{0.5}]$ where $I_0()$ is the modified Bessel function of the first kind, the following double integral results:

$$m^2 = 2.6056 C_n^2 k^2 \operatorname{Re} \left\{ |D(\mathbf{p}, L)|^{-2} \sum_{l_1=1}^N \sum_{l_2=1}^N A_{l_1} A_{l_2}^* e^{-i(\theta_{l_1}-\theta_{l_2})} \times \frac{1}{(1+i\alpha_{l_1} L)} \frac{1}{(1-i\alpha_{l_2}^* L)} \exp \left[-\frac{i(V_{xl_1}^2 + V_{yl_1}^2)L}{2k(1+i\alpha_{l_1} L)} + \frac{i[(V_{xl_2}^2)^* + (V_{yl_2}^2)^*]L}{2k(1-i\alpha_{l_2}^* L)} \right] \left[\int_0^L d\eta \int_0^\infty d\kappa \kappa^{-8/3} \times I_0 \left(\left\{ \left[\frac{i(L-\eta)V_{xl_1}}{k(1+i\alpha_{l_1} L)} - \frac{i(L-\eta)V_{xl_2}^*}{k(1-i\alpha_{l_2}^* L)} \right]^2 + \left[\frac{i(L-\eta)V_{yl_1}}{k(1+i\alpha_{l_1} L)} - \frac{i(L-\eta)V_{yl_2}^*}{k(1-i\alpha_{l_2}^* L)} \right]^2 \right\}^{0.5} \kappa \right) \times \exp \left\{ -0.5(L-\eta) \left[\frac{i(1+i\alpha_{l_1} \eta)}{k(1+i\alpha_{l_1} L)} - \frac{i(1-i\alpha_{l_2}^* \eta)}{k(1-i\alpha_{l_2}^* L)} \right] \kappa^2 \right\} \right] - D^{-2}(\mathbf{p}, L) \sum_{l_1=1}^N \sum_{l_2=1}^N A_{l_1} A_{l_2} e^{-i(\theta_{l_1}+\theta_{l_2})} \frac{1}{(1+i\alpha_{l_1} L)} \frac{1}{(1+i\alpha_{l_2} L)} \times \exp \left[-\frac{i(V_{xl_1}^2 + V_{yl_1}^2)L}{2k(1+i\alpha_{l_1} L)} - \frac{i(V_{xl_2}^2 + V_{yl_2}^2)L}{2k(1+i\alpha_{l_2} L)} \right] \times \left[\int_0^L d\eta \int_0^\infty d\kappa \kappa^{-8/3} I_0 \left(\left\{ \left[\frac{i(L-\eta)V_{xl_1}}{k(1+i\alpha_{l_1} L)} - \frac{i(L-\eta)V_{xl_2}}{k(1+i\alpha_{l_2} L)} \right]^2 + \left[\frac{i(L-\eta)V_{yl_1}}{k(1+i\alpha_{l_1} L)} - \frac{i(L-\eta)V_{yl_2}}{k(1+i\alpha_{l_2} L)} \right]^2 \right\}^{0.5} \kappa \right) \exp \left\{ -0.5(L-\eta) \left[\frac{i(1+i\alpha_{l_1} \eta)}{k(1+i\alpha_{l_1} L)} + \frac{i(1+i\alpha_{l_2} \eta)}{k(1+i\alpha_{l_2} L)} \right] \kappa^2 \right\} \right] \right\}, \quad (8)$$

In solving the integral over κ , the two modified Bessel functions of the first kind, $I_0()$, are expanded in series, then to each term of the series multiplied by the accompanying exponential, Eq. 3.478.1 of Ref. 22, which is $\int_0^\infty dx x^{\nu-1} \exp(-\mu x^p) = p^{-1} \mu^{-\nu/p} \Gamma(\nu/p)$ where Γ is the gamma function, is individually applied. After these developments, the scintillation index takes the following form:

$$\begin{aligned}
m^2 = & 1.3028 C_n^2 k^2 \operatorname{Re} \left[|D(\mathbf{p}, L)|^{-2} \sum_{l_1=1}^N \sum_{l_2=1}^N \sum_{r=0}^{\infty} A_{l_1} A_{l_2}^* \right. \\
& \times \exp[-i(\theta_{l_1} - \theta_{l_2})] \frac{1}{(1+i\alpha_{l_1}L)} \frac{1}{(1-i\alpha_{l_2}^*L)} \frac{(0.25)^r}{(r!)^2} \\
& \times \Gamma\left(r - \frac{5}{6}\right) \exp\left\{-\frac{i(V_{xl_1}^2 + V_{yl_1}^2)L}{2k(1+i\alpha_{l_1}L)} \right. \\
& \left. + \frac{i[(V_{xl_2}^2)^* + (V_{yl_2}^2)^*]L}{2k(1-i\alpha_{l_2}^*L)} \right\} \\
& \times \left(\int_0^L d\eta \left[\frac{i(L-\eta)V_{xl_1}}{k(1+i\alpha_{l_1}L)} - \frac{i(L-\eta)V_{xl_2}^*}{k(1-i\alpha_{l_2}^*L)} \right]^2 \right. \\
& \left. + \left[\frac{i(L-\eta)V_{yl_1}}{k(1+i\alpha_{l_1}L)} - \frac{i(L-\eta)V_{yl_2}^*}{k(1-i\alpha_{l_2}^*L)} \right]^2 \right)^r \\
& \times \left\{ 0.5(L-\eta) \left[\frac{i(1+i\alpha_{l_1}\eta)}{k(1+i\alpha_{l_1}L)} - \frac{i(1-i\alpha_{l_2}^*\eta)}{k(1-i\alpha_{l_2}^*L)} \right] \right\}^{-r+5/6} \Bigg) \\
& - D^{-2}(\mathbf{p}, L) \sum_{l_1=1}^N \sum_{l_2=1}^N \sum_{r=0}^{\infty} A_{l_1} A_{l_2} \exp[-i(\theta_{l_1} + \theta_{l_2})] \\
& \times \frac{1}{(1+i\alpha_{l_1}L)} \frac{1}{(1+i\alpha_{l_2}L)} \frac{(0.25)^r}{(r!)^2} \Gamma\left(r - \frac{5}{6}\right) \\
& \times \exp\left[-\frac{i(V_{xl_1}^2 + V_{yl_1}^2)L}{2k(1+i\alpha_{l_1}L)} - \frac{i(V_{xl_2}^2 + V_{yl_2}^2)L}{2k(1+i\alpha_{l_2}L)} \right] \\
& \times \left(\int_0^L d\eta \left[\frac{i(L-\eta)V_{xl_1}}{k(1+i\alpha_{l_1}L)} - \frac{i(L-\eta)V_{xl_2}}{k(1+i\alpha_{l_2}L)} \right]^2 \right. \\
& \left. + \left[\frac{i(L-\eta)V_{yl_1}}{k(1+i\alpha_{l_1}L)} - \frac{i(L-\eta)V_{yl_2}}{k(1+i\alpha_{l_2}L)} \right]^2 \right)^r \left\{ 0.5(L-\eta) \right. \\
& \left. \times \left[\frac{i(1+i\alpha_{l_1}\eta)}{k(1+i\alpha_{l_1}L)} + \frac{i(1+i\alpha_{l_2}\eta)}{k(1+i\alpha_{l_2}L)} \right] \right\}^{-r+5/6} \Bigg), \quad (9)
\end{aligned}$$

where ! denotes the factorial. As a check point, at the limits of $N=1$, $V_x=V_y=0$, meaning the Gaussian case, Eq. (9), when divided by 4, matches exactly Eqs. (18)–(29) of Ref. 14.

3. RESULTS AND DISCUSSION

We note that the scintillation index formula provided by Eq. (9) is able to account for any type of beam composed

from the summation of different fundamental Gaussian beams. In this study, however, we limit our attention to cos-Gaussian and annular beams and their comparison to pure Gaussian cases. From Eq. (9), the cos-Gaussian beam is attained by selecting $N=2$, $V_{xl}=V_{yl}=-V_x$ for the first beam, $V_{xl}=V_{yl}=V_x$ for the second beam, and making the rest of the source parameters the same in both the first and second terms of the summations. Annular beam is also constructed by taking two beams, i.e., $N=2$, called primary and secondary, but additionally by setting the source size in the secondary beam to be lower than that of the first beam, simultaneously equating the displacement parameters to zero. The amplitude factors for the cos-Gaussian beam are $A_l=(0.5, 0.5)$ while $A_l=(0.5, -0.5)$ for the annular beam. The phase parameter θ_l is taken zero for all situations. We produce graphs at a single value of structure constant, that is, $C_n^2=10^{-15} \text{ m}^{-2/3}$, which together with adapted values of the path length and the wavelength, make our results valid for the weak turbulent regime. The strength of turbulence is determined by the cumulative effect of the wavelength, propagation distance, and the structure constant. The regime of weak atmospheric turbulence is defined for situations¹⁵ where intensity fluctuations are relatively low. Specifically, we speak about weak turbulent regime, when the scintillations of a plane-wave incidence are less than unity, i.e., $1.23 C_n^2 k^{7/6} L^{11/6} < 1$. Since our formulation is based on the Rytov method, which yields a weak turbulence solution for the scintillation index, our results subsequently cover weak turbulence, i.e., in our plots, the values for k , L , and C_n^2 are chosen such that the weak turbulence condition $1.23 C_n^2 k^{7/6} L^{11/6} < 1$ is fulfilled. Also in our plots, unless stated otherwise, collimated beams are considered. As a general rule, our graphical illustrations will only quote the parameter values left unspecified here with the indexing being arranged to exclude the subscript l .

To aid comprehension of the subject, we initially show, in Fig. 1(a), the source plane intensities of the cos-Gaussian and Gaussian beams used in most of our graphs overlaid on the same contour plot. As described in our previous work,²³ the intensity of a cos-Gaussian beam will be divided into several lobes that are aligned with respect to the slanted axis. The number of lobes and their respective amplitudes will be determined by the displacement parameter present in the argument of the cosine function, and both will increase against growing displacement values. Due to the scale of source size and the displacement value employed, the side lobes of this particular cos-Gaussian beam are extremely weak compared to the central lobe as also seen from Fig. 1(b) that exhibits the 3D view of the cos-Gaussian beam of Fig. 1(a).

Figure 2 indicates how the differing levels of the displacement parameter affect the scintillation index, m^2 , along the propagation axis at selected values of source size and wavelength. The natural expectation that the scintillation index will rise with extending propagation distance is confirmed by Fig. 2. It is further realized from Fig. 2 that, in comparison to the Gaussian case for which $V_x=0 \text{ m}^{-1}$, at a source size of $\alpha_s=2 \text{ cm}$, the cos-Gaussian beam offers a range where the scintillation index values are smaller. This range extends from $L=0$ up to a point of intersection between the cos-Gaussian and Gaussian

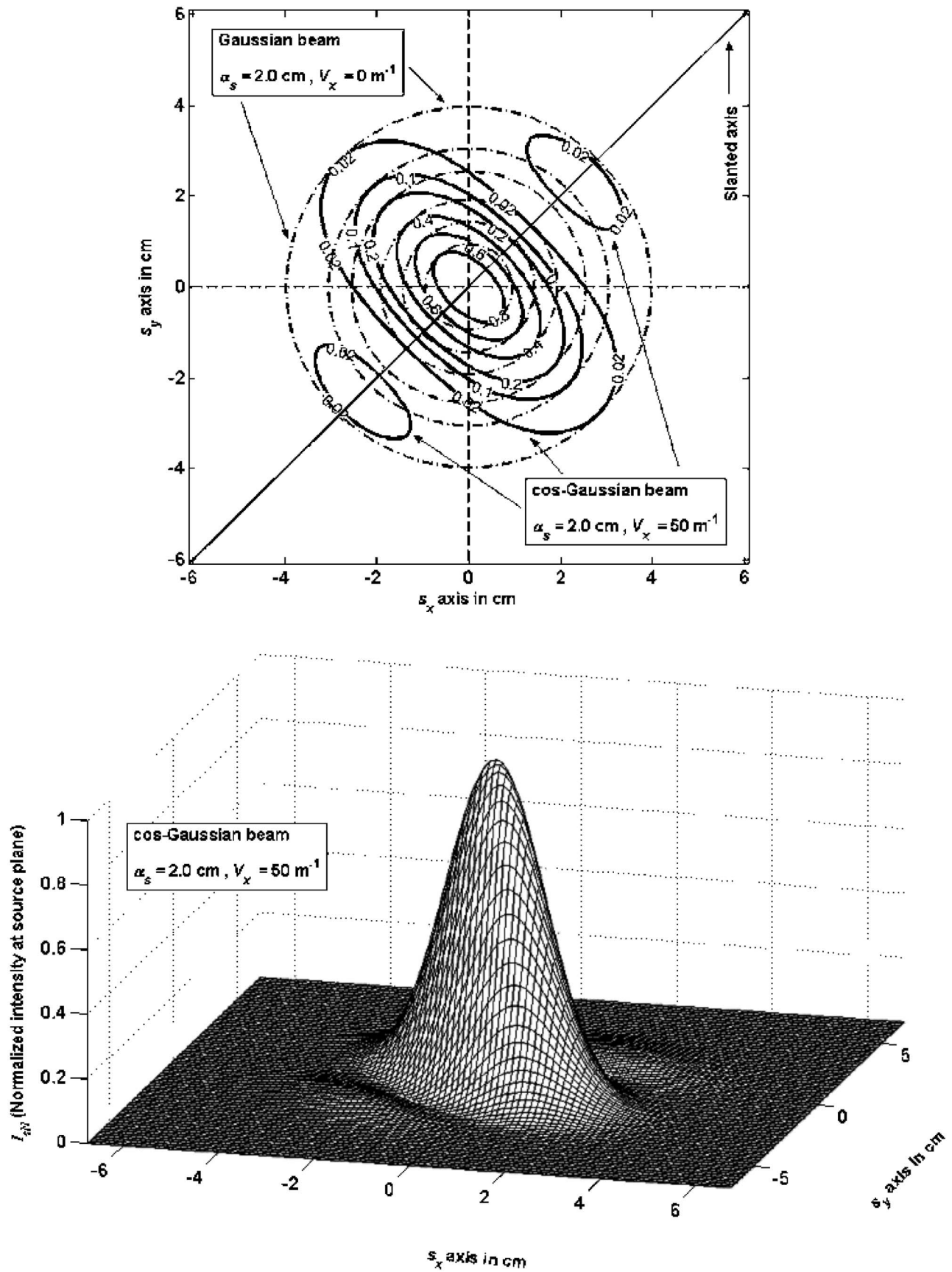


Fig. 1. (a) Contour plot of overlaid cos-Gaussian and Gaussian beams. (b) Three-dimensional normalized intensity of cos-Gaussian beam belonging to (a).

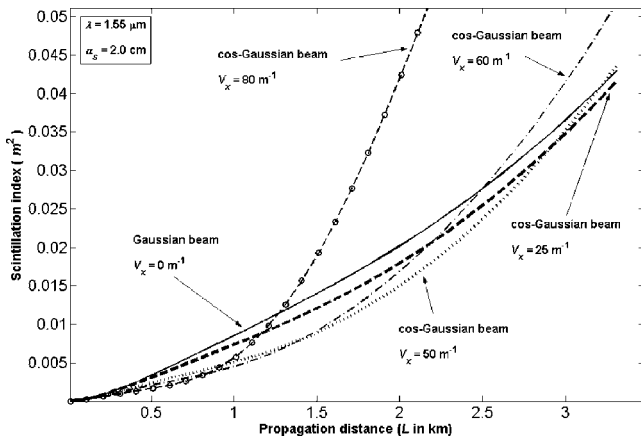


Fig. 2. Scintillation index of cos-Gaussian beam versus propagation distance at selected values of displacement parameters.

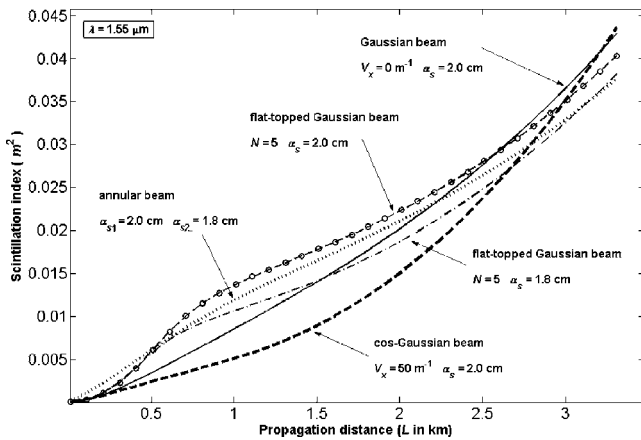


Fig. 3. Scintillation index for flat-topped, collimated annular, Gaussian, and cos-Gaussian beams versus propagation distance.

scintillation curves. According to Fig. 2, raising the displacement parameter will cause the scintillation index to attain lower values particularly at shorter propagation distances but simultaneously carrying the crossover point of cos-Gaussian and Gaussian beams scintillation curves toward earlier propagation distances. Viewed in this manner, for fixed source and propagation conditions, there appears to be an optimum threshold for the displacement parameter, which, in this instance, occurs at approximately $V_x = 1/\alpha_s$. Figure 3 is a plot of the scintillation index variation against the propagation distance for flat-topped, annular, Gaussian, and cos-Gaussian beams where the already studied flat-topped beams²⁰ are included for completeness. In Fig. 3, we have chosen the source size of one flat-topped beam, primary part of annular beam, Gaussian, and cos-Gaussian beams to be the same as Fig. 2, that is, $\alpha_{s1} = \alpha_s = 2$ cm, while the other flat-topped and the secondary part in the annular beam have a source size of $\alpha_{s2} = 1.8$ cm. In adapting Eq. (1) for flat-topped beams, the amplitude factor A_l has to be suitably adjusted so that it produces the amplitude coefficients in Eq. (7) of Ref. 20. The summation index n inside the exponential term of Eq. (7) of Ref. 20 is, on the other hand, to be incorporated into the α_x and α_y parameters of Eq. (1). Out of the two flat-topped beams of Fig. 3 plotted after

making these arrangements in Eq. (1), the flat-topped beam with $N=5$, $\alpha_s = 1.8$ cm exactly matches Fig. 3 of Ref. 20 for $N=5$. Figure 3 of the current paper demonstrates that, at the given source and propagation settings, in terms of the scintillation index, the cos-Gaussian beam retains the already mentioned property of being advantageous at short propagation distances, while the flat-topped and annular beams emerge to be beneficial particularly at longer propagation distances. We note that these observations regarding the behaviors of flat-topped and the annular beams are in line with the conclusions of Refs. 20 and 17, respectively. Next, we explore the effect of focusing parameter excluding the flat-topped beams. In this context Fig. 4 shows that, when the focusing parameter of $F=1$ km (note that for all the beams $F=F_x=F_y$) is included in the beams, the curves of Fig. 3 become almost reversed after approximately $L=800$ m where the scintillation index of the annular beam becomes the lowest while that of the cos-Gaussian beam is the highest. As understood from the combined examination of Figs. 3 and 4, however, a focused beam will serve to obtain smaller scintillations. This behavior concerning the Gaussian case only is also reported in Ref. 17.

Figure 5 displays the dependency of the scintillation index for the cos-Gaussian beam on the wavelength of operation versus the displacement parameter. It is seen from Fig. 5 that lower wavelengths will give rise to higher scintillation indexes. On the other hand, decreasing wavelengths appear to push the optimum value of the displacement parameter for achieving the lowest scintillation index values, mentioned in relation to Fig. 2, toward bigger values of the displacement parameter. The corresponding scintillation indices of pure Gaussian beams can be read directly from the vertical axis of Fig. 5, that is, $V_x=0$ points of the horizontal axis.

The course of scintillation index for Gaussian, cos-Gaussian, and annular beams at two propagation lengths of $L=1$ and $L=2.5$ km, against the continually changing source size, is analyzed in Fig. 6 where the vertical logarithm-axis is utilized for ease of distinction between beams. In the graphs of Fig. 6, we have arranged the displacement parameter of cos-Gaussian beams to be the inverse of the respective source size, that is, $V_x=1/\alpha_s$ and for annular beams, $\alpha_{s2}/\alpha_{s1}=0.9$, while in the case of an-

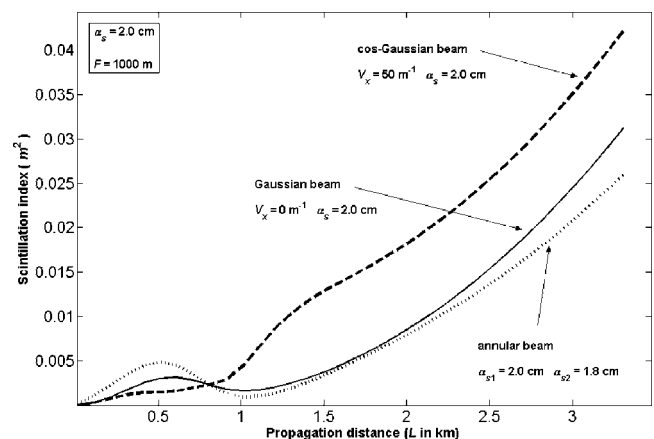


Fig. 4. Scintillation index for focused annular, Gaussian, and cos-Gaussian beams versus propagation distance.

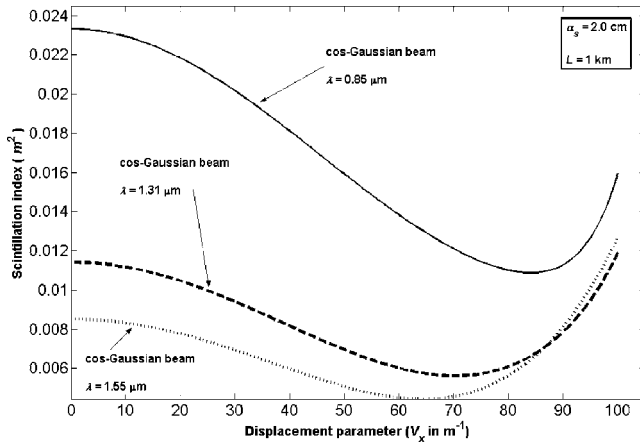


Fig. 5. Scintillation index of cos-Gaussian beam versus displacement distance at selected values of wavelengths of operation.

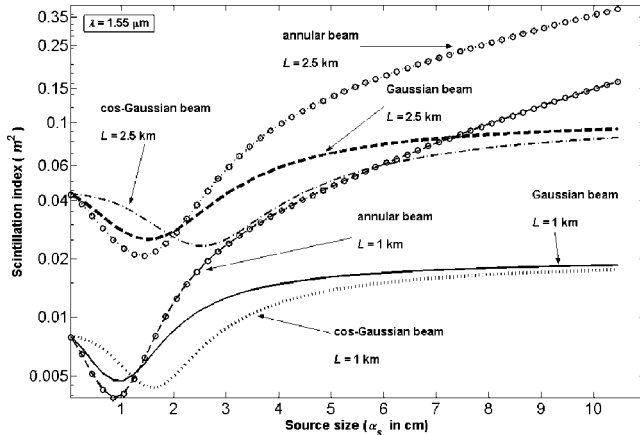


Fig. 6. Scintillation index of Gaussian and cos-Gaussian beams versus source size at selected values of propagation lengths.

nular beams, the horizontal axis refers to the source size of the primary beam. It is detected from Fig. 6 that, since they provide lower scintillations, cos-Gaussian beams are specifically advantageous at relatively large source sizes; whereas the reverse holds for the annular beams. In fact, as the source size gets bigger, the scintillation index of annular beams escalates to excessively large values. Moreover, the advantageous region of the cos-Gaussian beam begins to cover the smaller source sizes if shorter propagation distances are considered. Figure 6 additionally reveals that the scintillation features of the pure Gaussian beam are typical also for cos-Gaussian beams. That is, the scintillation index will initially display a downward trend at small source sizes but after reaching a dip, will start to increase, eventually approaching the well-known plane-wave limit²⁴ for relatively large source sizes. The annular beams, on the other hand, exhibit different characteristics at large source sizes. This is because for an annular beam, to approach the plane-wave limit, the source size of the primary beam should be allowed to go to infinity, while that of the secondary beam should be allowed to go to zero. It is easy to realize that the chosen annular beams of Fig. 6 have fixed source size ratios hence not conforming to this configuration.

4. CONCLUSION

With the aid of generalized beam formulation, we have examined and made comparisons between the scintillation index characteristics of flat-topped, collimated, and focused cos-Gaussian and annular beams in turbulence. These comparisons show that a cos-Gaussian beam (collimated) and annular beam (collimated and focused), flat-topped (collimated) offer certain advantages over their counterpart of a pure Gaussian beam, respectively, at shorter and longer propagation distances.

For the cos-Gaussian beam, a larger displacement parameter makes the scintillations smaller than the scintillations of the corresponding Gaussian beam at shorter link lengths; whereas this behavior is reversed for longer link lengths. A certain threshold value of the displacement parameter is encountered here beyond which no substantial improvements in the scintillations of cos-Gaussian beam can be obtained. Annular beams both in collimated and focused forms seem to be attractive especially at longer propagation distances.

As expected, the scintillations for cos-Gaussian and annular beams are higher for lower wavelengths. An additional observation is that at a fixed link length the optimum value of the displacement parameter for achieving lowest scintillation indices is shifted toward bigger values at smaller wavelengths.

Viewed against the source size changes, the cos-Gaussian beam almost entirely follows the characteristics of the pure Gaussian case, that is, initially high scintillations at small source sizes, then exhibiting a dip at moderate source sizes and eventually rising to reach plane-wave limits at relatively large source sizes. Source size variation plots also demonstrate that to obtain lower scintillations, cos-Gaussian beams of relatively large source sizes should be preferred.

H. T. Eyyuboğlu's e-mail address is h.eyyuboglu@cankaya.edu.tr; phone: (+90) 312-284-4500/360; fax: (+90) 312-284-8043.

Y. K. Baykal's e-mail address is y.baykal@cankaya.edu.tr; phone: (+90) 312-284-4500/262; fax: (+90) 312-284-8043.

REFERENCES

1. L. C. Andrews, R. L. Phillips, C. Y. Hopen, and M. A. Al-Habash, "Theory of optical scintillation," *J. Opt. Soc. Am. A* **16**, 1417–1429 (1999).
2. L. C. Andrews, M. A. Al-Habash, C. Y. Hopen, and R. L. Phillips, "Theory of optical scintillation: Gaussian-beam wave model," *Waves Random Media* **11**, 271–291 (2001).
3. V. A. Banakh and V. L. Mironov, "Influence of the diffraction size of a transmitting aperture and the turbulence spectrum on the intensity fluctuations of laser radiation," *Sov. J. Quantum Electron.* **8**, 875–878 (1978).
4. W. B. Miller, J. C. Ricklin, and L. C. Andrews, "Effects of the refractive index spectral model on the irradiance variance of a Gaussian beam," *J. Opt. Soc. Am. A* **11**, 2719–2726 (1994).
5. G. Ya. Patrushev, "Fluctuations of the field of a wave beam on reflection in a turbulent atmosphere," *Sov. J. Quantum Electron.* **8**, 1315–1318 (1978).
6. R. L. Fante, "Comparison of theories for intensity fluctuations in strong turbulence," *Radio Sci.* **11**, 215–220 (1976).
7. K. S. Gochelashvili, V. G. Pevgov, and V. I. Shishov,

- “Saturation of fluctuations of the intensity of laser radiation at large distances in a turbulent atmosphere,” *Sov. J. Quantum Electron.* **4**, 632–637 (1974).
8. S. I. Belousov and I. G. Yakushkin, “Strong fluctuations of fields of optical beams in randomly inhomogeneous media,” *Sov. J. Quantum Electron.* **10**, 301–304 (1980).
 9. V. A. Banakh, G. M. Krekov, V. L. Mironov, S. S. Khmelevtsov, and R. Sh. Tsvik, “Focused-laser-beam scintillations in the turbulent atmosphere,” *J. Opt. Soc. Am.* **64**, 516–518 (1974).
 10. F. S. Vetelino, C. Young, L. C. Andrews, K. Grant, K. Corbett, and B. Clare, “Scintillation: theory vs. experiment,” in *Atmospheric Propagation II*, C. Y. Young and G. C. Gilbreath, eds., *Proc. SPIE* **5793**, 166–177 (2005).
 11. J. C. Ricklin and F. M. Davidson, “Atmospheric optical communication with a Gaussian–Schell beam,” *J. Opt. Soc. Am. A* **20**, 856–866 (2003).
 12. O. Korotkova, “Control of the intensity fluctuations of random electromagnetic beams on propagation in weak atmospheric turbulence,” in *Free-Space Laser Communication Technologies XVIII*, G. S. Mecherle, ed., *Proc. SPIE* **6105**, 61050V (2006).
 13. V. I. Tatarski, *Wave Propagation in a Turbulent Medium* (McGraw-Hill, 1961).
 14. A. Ishimaru, *Wave Propagation and Scattering in Random Media* (Academic, 1978), Vol. 2.
 15. L. C. Andrews and R. L. Phillips, *Laser Beam Propagation through Random Media* (SPIE, 2005).
 16. L. C. Andrews, R. L. Phillips, and C. Y. Hopen, *Laser Beam Scintillation with Applications* (SPIE, 2001).
 17. F. S. Vetelino and L. C. Andrews, “Annular Gaussian beams inturbulent media,” in *Free-Space Laser Communication and Active Laser Illumination III*, D. G. Voelz and J. C. Ricklin, eds., *Proc. SPIE* **5160**, 86–97 (2004).
 18. D. C. Cowan, J. Reclons, L. C. Andrews, and C. Y. Young, “Propagation of flattened Gaussian beams in the atmosphere: a comparison of theory with a computer simulation model,” in *Atmospheric Propagation III*, C. Y. Young and G. C. Gilbreath, eds., *Proc. SPIE* **6215**, 62150B (2006).
 19. Y. Baykal, “Formulation of correlations for general-type beams in atmospheric turbulence,” *J. Opt. Soc. Am. A* **23**, 889–893 (2006).
 20. Y. Baykal and H. T. Eyyubođlu, “Scintillation index of flat-topped-Gaussian beams,” *Appl. Opt.* **45**, 3793–3797 (2006).
 21. Y. Baykal, “Beams with arbitrary field profiles in turbulence,” in *SPIE Conference, XIII International Symposium on Atmospheric and Ocean Optics. Atmospheric Physics* (Tomsk, Russia, July 2–7, 2006), invited paper.
 22. I. S. Gradshteyn and I. M. Ryzhik, *Tables of Integrals, Series and Products* (Academic, 2000).
 23. H. T. Eyyubođlu and Y. Baykal, “Analysis of reciprocity of cos-Gaussian and cosh-Gaussian laser beams in turbulent atmosphere,” *Opt. Express* **12**, 4659–4674 (2004).
 24. A. Ishimaru, “Fluctuations in the parameters of spherical waves propagating in a turbulent atmosphere,” *Radio Sci.* **4**, 295–305 (1969).